Induced α Helix in the VP16 Activation Domain upon Binding to a Human TAF

Motonari Uesugi, Origène Nyanguile, Hua Lu, Arnold J. Levine, Gregory L. Verdine*

Activation domains are functional modules that enable sequence-specific DNA binding proteins to stimulate transcription. The structural basis for the function of activation domains is poorly understood. A combination of nuclear magnetic resonance (NMR) and biochemical experiments revealed that the minimal acidic activation domain of the herpes simplex virus VP16 protein undergoes an induced transition from random coil to α helix upon binding to its target protein, $hTAF_{II}31$ (a human TFIID TATA box–binding protein-associated factor). Identification of the two hydrophobic residues that make nonpolar contacts suggests a general recognition motif of acidic activation domains for $hTAF_{II}31$.

Activation of transcription in eukaryotes is directed by regulatory proteins that recruit the transcriptional machinery and chromatin remodeling factors to the promoter. Typically, these regulatory proteins are modular, having distinct domains for sequence-specific binding to DNA and for transcriptional activation through interactions with other proteins (*1*). Activation domains are classified according to the preponderance of amino acid residues such as glutamine, proline, and those bearing acidic side chains. Of these classes, the acidic activators have been the most extensively studied (*2*). Notwithstanding the gains that have been made in identifying the targets of acidic activation domains (*1*) and elucidating the importance of particular residues for their function (*3*), the structural basis for the ability of activation domains to stimulate transcription remains poorly understood (*2*, *4*). Here, we report that the activation domain of the herpes simplex virus VP16 protein undergoes an induced coil-to-helix transition upon interaction with its target protein $hTAF_{II}31$, with residues along one face of the nascent helix making intermolecular contacts to $hTAF_{II}31$.

The acidic activation domains of VP16 and tumor suppressor p53 directly target $hTAF_{II}31$ and its *Drosophila* homolog, $dTAF_{II}40$; the strength of this interaction correlates with the ability to activate transcription in vitro (5–7). The molecular interaction has been mapped to the NH_2-terminal 181 amino acids of $hTAF_{II}31$ (TAF_{1-181}) and a COOH-terminal segment of the VP16 activation domain ($VP16_C$, residues 452 to 490) (5). Because the stability of TAF_{1-181} is poor, we overexpressed a smaller fragment, TAF_{1-140}, which comprises the region of highest homology to $dTAF_{II}40$ (*8*) and binds $VP16_C$ as tightly as does TAF_{1-181} (9). TAF_{1-140} was soluble up to ~300 μM in pH 6.2 buffer and thus was deemed suitable for NMR studies.

To analyze the interaction between TAF_{1-140} and $VP16_C$, we performed ^1H-^{15}N heteronuclear single-quantum coherence (HSQC) NMR experiments with ^{15}N-labeled $VP16_C$ and varying amounts of unlabeled TAF_{1-140} (*10*). The enrichment of $VP16_C$ with ^{15}N permitted selective detection of signals from $VP16_C$, but not from unlabeled TAF_{1-140}. The limited dispersion of the backbone ^{15}N and ^1HN chemical shifts in the HSQC spectrum of ^{15}N-labeled $VP16_C$ alone (Fig. 1A) and the intermediate values (~7 Hz) of ^1HN-$^1HC^\alpha$ coupling constants (*11*) indicated that $VP16_C$ alone has negligible secondary structure (*12*). Titration of ^{15}N-labeled $VP16_C$ with unlabeled TAF_{1-140} resulted in progressive rather than bimodal changes of the backbone ^{15}N and ^1HN chemical shifts (Fig. 1A), thus indicating that $VP16_C$ interacts weakly with TAF_{1-140} and hence exchanges rapidly between the free and bound states on the NMR time scale (*13*). Sequential assignment of the HSQC cross-peaks (*14*) established that the backbone-perturbed residues are located within a region at the COOH-terminal end of $VP16_C$ that encompasses residues 475 to 484 (Fig. 1B).

Gross changes in backbone chemical shifts can generally be ascribed to global alterations in folded structure. To assess the importance of the side chains, we analyzed the chemical shift perturbations of the β protons in $VP16_C$ upon complexation with TAF_{1-140} (*15*). Significant chemical shift changes were observed only for the β protons of Asp^{472}, Phe^{479}, Leu^{483}, and Asp^{486} (Fig. 1C). These four residues lie within and adjacent to the region of $VP16_C$ that is suggested by backbone chemical shift perturbation to undergo an induced folding transition.

To analyze independently the importance of residues in $VP16_C$ for both the interaction with TAF_{1-140} and activation of transcription, we performed in vitro biochemical assays with a series of $VP16_C$ deletion mutant proteins (Fig. 2A). For detection of TAF-binding activity, each deletion mutant was fused to glutathione-S-transferase (GST) and analyzed for the ability to pull down TAF_{1-140} (Fig. 2B) (*16*). Deletion of residues 475 to 490 from GST-$VP16_C$ abolished TAF binding, whereas deletion of residues 452 to 468 retained binding activity. Further deletion of residues 486 to 490 had no detectable effect; however, removal of residues 469 to 473 or 481 to 485 resulted in a loss of binding activity. For assessment of the ability of the deletion mutants to activate transcription, each mutant was fused to the yeast GAL4 DNA binding domain (residues 1 to 147) and analyzed for the ability to activate transcription in vitro with HeLa nuclear extracts (Fig. 2C) (*17*). GAL4-$VP16_C$ stimulated transcription of the reporter construct containing five GAL4 recognition sites (5). A fusion construct in which residues 452 to 468 of $VP16_C$ were deleted activated transcription as strongly as did GAL4-$VP16_C$ itself. However, deletion of residues 475 to 490 reduced activation potential; this was slightly above GAL4 activation alone. Although deletion of residues 486 to 490 had no detectable effect, further deletion of residues 469 to 473 or 481 to 485 reduced transcriptional activity. Thus, the transcriptional activity of $VP16_C$ is directly correlated with the strength of its binding to TAF_{1-140}; this is consistent with the notion that the interaction between these two proteins is responsible for the activation signal observed in our in vitro assays. Moreover, the COOH-terminal segment of $VP16_C$ ($VP16_{469-485}$, residues 469 to 485) is necessary and sufficient to bind TAF_{1-140} and activate transcription in vitro, and it corresponds to the region that was mapped through NMR experiments to interact with TAF_{1-140}.

To determine the structure of $VP16_{469-485}$ bound to TAF_{1-140}, we performed transferred nuclear Overhauser effect (TRNOE) experiments. TRNOE relies on rapid exchange between the free and bound states for a relatively small ligand in the presence of its macromolecular receptor. Under conditions of rapid exchange, negative NOEs conveying conformational information about the bound ligand are transferred to the resonances of the free ligand (*18*). In the ideal case, NOEs from

M. Uesugi, O. Nyanguile, G. L. Verdine, Department of Chemistry and Chemical Biology, Harvard University, Cambridge, MA 02138, USA.
H. Lu and A. J. Levine, Department of Molecular Biology, Princeton University, Princeton, NJ 08544, USA.
*To whom correspondence should be addressed.

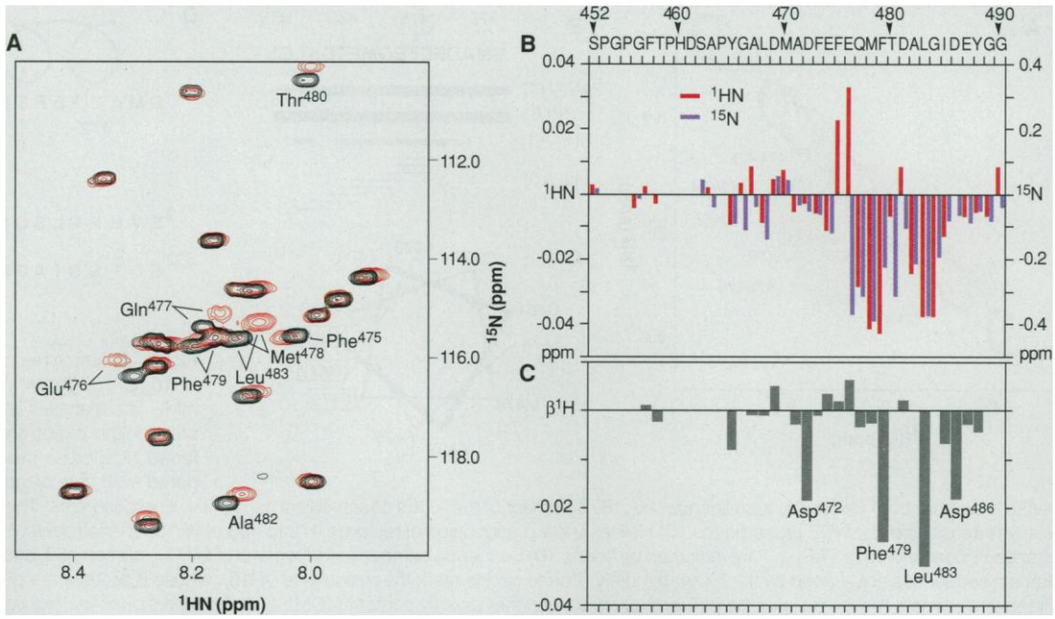

Fig. 1. (**A**) Expanded ^{1}H-^{15}N HSQC spectra of ^{15}N-labeled $VP16_C$ (900 μM) in the absence (black) or presence (red) of TAF_{1-140} (300 μM). Significantly shifted cross-peaks are indicated. Glycine cross-peaks are not shown; the cross-peak from Gly^{484} shifted in the presence of TAF_{1-140}. (**B** and **C**) Histogram showing ^{1}HN and ^{15}N (B) and $\beta^{1}H$ (C) chemical shift changes in $VP16_C$ induced by binding of TAF_{1-140}. The positions of amino acids are indicated. Chemical shifts of the β protons were determined by ^{1}H-^{15}N NOESY-HSQC and ^{1}H-^{15}N TOCSY-HSQC experiments. When diastereotopic β-proton signals were observed, only the chemical shift change of the proton having the largest effect is indicated. Abbreviations for the amino acid residues are as follows: A, Ala; C, Cys; D, Asp; E, Glu; F, Phe; G, Gly; H, His; I, Ile; K, Lys; L, Leu; M, Met; N, Asn; P, Pro; Q, Gln; R, Arg; S, Ser; T, Thr; V, Val; W, Trp; and Y, Tyr.

the free ligand itself approach zero because of its low molecular weight; hence, NOEs can be detected primarily from the bound ligand in the presence of a substoichiometric amount of the receptor. As anticipated, free $VP16_{469-485}$ exhibited very few NOEs; only sequential NOEs between $C^{\alpha}H$ and NH protons [$d_{\alpha N}(i,i+1)$ NOEs] were clearly observed, indicative of an extended random-coil structure (*19*). In contrast, $VP16_{469-485}$ in the presence of 0.1 mole equivalents of TAF_{1-140} showed numerous NOE cross-peaks, including a substantial number arising from $d_{NN}(i,i+1)$, $d_{\alpha N}(i,i)$, and $d_{\alpha\beta}(i,i+3)$ NOEs. The overall pattern of the NOE connectivities (Fig. 3B) is characteristic of that observed for α-helical secondary structure, especially in the region from Asp^{472} to Leu^{483}. Thus, residues 472 to 483 of $VP16_C$, and perhaps even residues flanking this region, adopt an α-helical structure when bound to TAF_{1-140} (*20*).

The projection of residues 472 to 483 of the VP16 activation domain onto a helical wheel is shown in Fig. 3C. Three of the four residues whose side chain β protons are perturbed upon binding to TAF_{1-140} lie along one face of the helix. These three residues—Asp^{472}, Phe^{479}, and Leu^{483}—may directly contact chemically complementary residues of TAF_{1-140}. Consistent with this idea, replacement of Phe^{479} and Leu^{483} with Ala reduced TAF_{1-140} binding affinity and transcriptional activation (Fig. 2, B and C, respectively) (*21*). Whereas Phe^{479} and Leu^{483} of $VP16_C$ presumably make hydrophobic contacts to TAF_{1-140}, Asp^{472} may participate in salt-bridge or hydrogen-bonding interactions. The fourth residue that exhibits β-proton chemical shift perturbation upon binding to TAF_{1-140}, Asp^{486}, can be deleted without significant loss of binding or transcriptional activation. This suggests that Asp^{486} makes little energetic

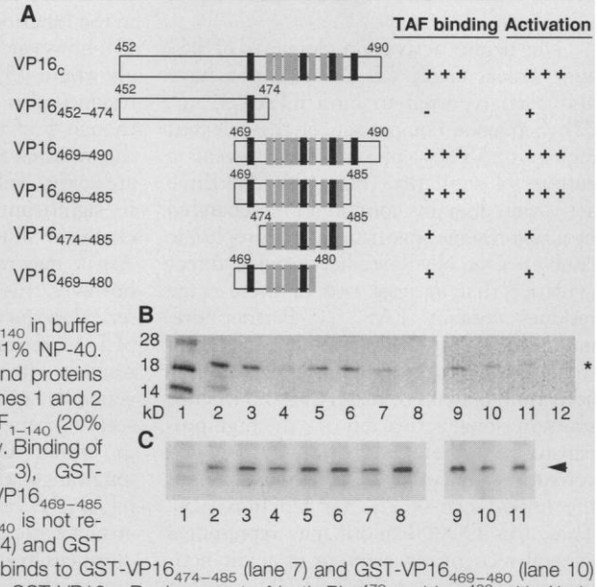

Fig. 2. In vitro biochemical experiments. (**A**) Schematic representation of VP16 deletion mutant proteins used for in vitro protein-protein interaction and transcription assays. Residues whose backbone NH chemical shifts (light gray) and β proton chemical shifts (black) were significantly changed upon binding to TAF_{1-140} are indicated. (**B**) In vitro protein-protein interaction assays. GST and GST-VP16 beads were incubated with TAF_{1-140} in buffer containing 50 mM NaCl and 0.01% NP-40. After extensive washing, the bound proteins were resolved by SDS-PAGE. Lanes 1 and 2 show the protein markers and TAF_{1-140} (20% of the input TAF_{1-140}), respectively. Binding of TAF_{1-140} to GST-$VP16_C$ (lane 3), GST-$VP16_{469-490}$ (lane 5), and GST-$VP16_{469-485}$ (lanes 6 and 9) is evident. TAF_{1-140} is not retained on GST-$VP16_{452-474}$ (lane 4) and GST (lanes 8 and 12) resins. TAF_{1-140} binds to GST-$VP16_{474-485}$ (lane 7) and GST-$VP16_{469-480}$ (lane 10) resins much more weakly than to GST-$VP16_C$. Replacement of both Phe^{479} and Leu^{483} with Ala in GST-$VP16_{469-485}$ (lane 11) greatly reduced binding affinity. The position of TAF_{1-140} is indicated by an asterisk. (**C**) In vitro transcription assays. Transcriptional activation by GAL4-VP16 mutant proteins was assayed in HeLa nuclear extracts. The reactions contained 2 pmol of the purified proteins and 100 ng of G_5BCAT template containing the adenovirus E1b promoter linked to five GAL4 recognition sites. The products of the transcription reactions were analyzed by primer extension. Lane 1 shows basal transcription without GAL4 proteins. Transcriptional activation by GAL4-$VP16_C$ (lane 3), GAL4-$VP16_{469-490}$ (lane 5), and GAL4-$VP16_{469-485}$ (lanes 6 and 9) is greater than that observed for GAL4 alone (lane 2). GAL4-$VP16_{452-474}$ (lane 4), GAL4-$VP16_{474-485}$ (lane 7), and GAL4-$VP16_{469-480}$ (lane 10) activate transcription much less than does GAL4-$VP16_C$ (lane 3). Lane 8 shows activated transcription by GAL4-$VP16_{NC}$, which contains both the NH_2-terminal and COOH-terminal subdomains (residues 413 to 490) of the VP16 activation domain. Replacement of both Phe^{479} and Leu^{483} with Ala greatly reduced transcriptional activation (lane 11). The position of the extension products is indicated by an arrowhead. The weak activation signal generated by $GAL4_{1-147}$ (lane 2) has been observed previously (*25*).

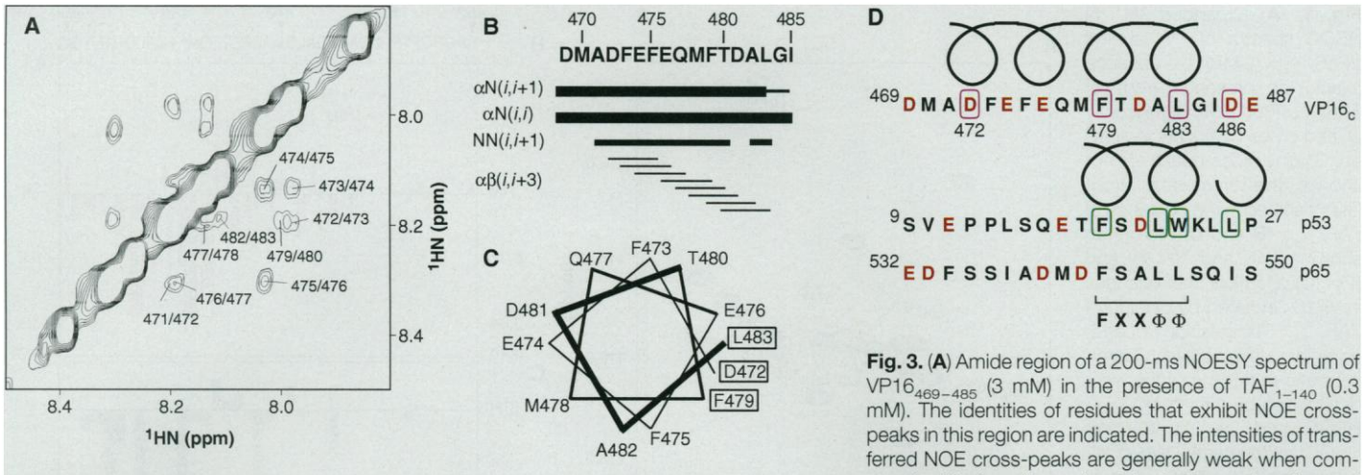

Fig. 3. (**A**) Amide region of a 200-ms NOESY spectrum of $VP16_{469-485}$ (3 mM) in the presence of TAF_{1-140} (0.3 mM). The identities of residues that exhibit NOE cross-peaks in this region are indicated. The intensities of transferred NOE cross-peaks are generally weak when compared with the diagonal peaks because the diagonal peaks arise from both free and bound ligands (*26*). (**B**) Summary of the NOEs observed from the TRNOE experiments. The thickness of the lines indicates the relative intensities of the NOE cross-peaks. (**C**) Helical wheel presentation of residues 472 to 483 of VP16. The residues whose β-proton chemical shifts were changed upon binding to TAF_{1-140} are indicated by boxes. (**D**) Sequence comparison of regions of $VP16_C$, human p53, and human NF-κB p65. The activation domain sequences are aligned by the FXXΦΦ moiety. Purple circles mark the residues of $VP16_C$ whose β protons are perturbed upon binding to TAF_{1-140}. Green circles mark the residues of the p53 activation domain that directly contact MDM2 (*23*). Acidic residues are highlighted in red. Although the β-proton chemical shift of Asp^{486} was significantly perturbed upon binding to TAF_{1-140}, the present biochemical experiments indicate that Asp^{486} is not essential for TAF binding and transcriptional activation. Black coils above the sequences of $VP16_C$ and p53 represent the regions over which α helix induction is observed upon binding to TAF_{1-140} and MDM2, respectively. Amino acid abbreviations are as in Fig. 1.

contribution to the protein-protein interaction, or possibly that the new COOH-terminal carboxyl generated through truncation functionally replaces the Asp^{486} side chain.

The acidic activation domains of p53 and nuclear factor κB (NF-κB) p65 have also been reported to bind $hTAF_{II}31$ (*6*, *22*). Sequence comparison of the relevant regions of $VP16_C$, p53, and p65 reveals a pattern of similarity (Fig. 3D): All three activation domains contain a Phe separated by a two-residue spacer from a hydrophobic doublet. Our NMR studies provide direct evidence that at least two of these three residues contact TAF_{1-140}. Furthermore, mutation of the hydrophobic residues in this motif abrogates binding of the p53 activation domain to $hTAF_{II}31$ and in vitro transcriptional activation (*6*); the high propensity of α helix formation by the p65 activation domain has been noted, as has the importance of Phe for function (*23*). Thus, this FXXΦΦ motif may represent a general recognition element of acidic activation domains for $TAF_{II}31$. The recent crystal structure of the p53 activation domain bound to the attenuator protein MDM2 reveals that the segment containing the FXXΦΦ moiety folds to form an α helix, from which the three hydrophobic residues project to make nonpolar contacts with MDM2 (*24*). Our study provides support for the hypothesis that the MDM2-p53 interaction mimics that of $TAF_{II}31$–acidic activation domains, even though MDM2 and $TAF_{II}31$ appear to be structurally unrelated (*22*, *24*).

A long-standing puzzle relates to the specific role of the acidic residues in the acidic activation domain. Evidence suggests that acidic residues play an important role in the function of acidic activation domains (*3*); however, the results presented here and elsewhere (*3*) indicate that hydrophobic residues also play an important role. Although 5 of the 17 residues that make up the minimal activation peptide $VP16_{469-485}$ are acidic, only one of these, Asp^{472}, exhibits significant perturbation of its β-proton chemical shift upon binding to TAF_{1-140}. Asp^{472} may make a direct, specific contact; however, this contact is apparently not conserved in the activation domains of p53 and p65. Moreover, the positions of the acidic residues in acidic activation domains generally appear to be unimportant. This seeming paradox can be resolved by a model in which the acidic residues establish long-range electrostatic interactions with $hTAF_{II}31$. Such electrostatic forces would attract basic $hTAF_{II}31$ over relatively long distances in solution, thereby increasing the rate at which the activation domain locates its target. Once the activation domain and $hTAF_{II}31$ come into close range, the activation domain undergoes an induced structural transition to an α helix, thereby enabling the establishment of direct hydrophobic contacts with nonpolar residues of $hTAF_{II}31$. Because such folding transitions are highly cooperative, the coupling of folding to targeting by activation domains provides a mechanism whereby multiple weak interactions can produce a pronounced biologic response.

REFERENCES AND NOTES

1. R. Tjian and T. Maniatis, *Cell* **77**, 5 (1994); B. F. Pugh, *Curr. Opin. Cell Biol.* **8**, 303 (1996).
2. S. J. Triezenberg, *Curr. Opin. Genet. Dev.* **5**, 190 (1995).
3. W. D. Cress and S. J. Triezenberg, *Science* **251**, 87 (1991); S. G. Roberts, I. Ha, E. Maldonado, D. Reinberg, M. R. Green, *Nature* **363**, 741 (1993); J. L. Regier, F. Shen, S. J. Triezenberg, *Proc. Natl. Acad. Sci. U.S.A.* **90**, 883 (1993); K. K. Leuther, J. M. Salmeron, S. A. Johnston, *Cell* **72**, 575 (1993); H. Moriuchi *et al.*, *Proc. Natl. Acad. Sci. U.S.A.* **92**, 9333 (1995).
4. P. O'Hare and G. Williams, *Biochemistry* **31**, 4150 (1992); L. Donaldson and J. P. Capone, *J. Biol. Chem.* **267**, 1411 (1992); F. Shen, S. J. Triezenberg, P. Hensley, D. Porter, J. R. Knutson, *ibid.* **271**, 4827 (1996).
5. J. A. Goodrich, T. Hoey, C. J. Thut, A. Admon, R. Tjian, *Cell* **75**, 519 (1993); R. D. Klemm, J. A. Goodrich, S. Zhou, R. Tjian, *Proc. Natl. Acad. Sci. U.S.A.* **92**, 5788 (1995).
6. C. J. Thut, J.-L. Chen, R. Klemm, R. Tjian, *Science* **267**, 100 (1995); H. Lu and A. J. Levine, *Proc. Natl. Acad. Sci. U.S.A.* **92**, 5154 (1995).
7. TAFs are apparently essential mediators of the transcriptional response to activation domains in metazoan cells [F. Sauer, D. A. Wassarman, G. M. Rubin, R. Tjian, *Cell* **87**, 1271 (1996); M. Hampsey and D. Reinberg, *Curr. Biol.* **7**, 44 (1997)], whereas activation domains may use other targets in yeast [S. S. Walker, J. C. Reese, L. M. Apone, M. R. Green, *Nature* **383**, 185 (1996); Z. Moqtaderi, Y. Bai, D. Poon, P. A. Weil, K. Struhl, *ibid.*, p. 188]. No known homolog of $hTAF_{II}31$ has been identified in yeast.
8. The DNA encoding each TAF fragment was generated as an Eco RI–Hind III DNA fragment with the polymerase chain reaction (PCR), cloned into the *Escherichia coli* vector pLM1 [K. D. MacFerrin, L. Chen, M. P. Terranova, S. L. Schreiber, G. L. Verdine, *Methods Enzymol.* **217**, 79 (1993)], and expressed in the host bacterial strain BL21 (DE3) pLysS. Cells were grown at 37°C to an optical density at 600 nm (OD_{600}) of 0.2 and then at 30°C to OD_{600} of 0.5 in 1 liter of media. The culture was then induced with 0.4 mM isopropyl-β-D-thiogalactopyranoside (IPTG) and harvested 5 hours later. The lysed bacterial mixture [10 mM tris-HCl (pH 7.4), 400

mM NaCl, and 10 mM phenylmethylsulfonyl fluoride (PMSF)] was centrifuged at 30,000*g* for 20 min. To the supernatant (10 ml) was added 0.5 ml of 5% polyethyleneimine. After swirling on ice, the sample was centrifuged at 30,000*g* for 20 min. The proteins in the supernatant were precipitated with ammonium sulfate. Each TAF fragment was purified using SP Sepharose and Q Sepharose columns (Pharmacia) and characterized by electrospray ionization mass spectroscopy. NMR spectra of TAF_{1-140} alone showed unexpectedly broad peaks, presumably attributable to dimer formation of the histone homology region [X. Xie *et al.*, *Nature* **380**, 316 (1996); A. Hoffmann *et al.*, *ibid.*, p. 356]. This broadening made it impractical to pursue NMR studies of TAF_{1-140} alone.

9. The ability of the TAF fragments to bind to $VP16_C$ was estimated by GST pull-down assays. GST-$VP16_C$ beads (loaded with 200 μg of protein) were incubated with 50 μg of each TAF fragment in 200 μl of binding buffer [20 mM tris-HCl (pH 7.4), 50 mM NaCl, 2 mM dithiothreitol (DTT), 10 mM $MgCl_2$, 0.01% NP-40, and 10% glycerol] at 4°C for 1 hour, and then washed five times with 200 μl of the same buffer. The samples were dissolved in SDS–polyacrylamide gel electrophoresis (PAGE) loading buffer and analyzed by SDS-PAGE.
10. The DNA encoding $VP16_C$ was generated as a Bam HI–Eco RI DNA fragment with PCR and cloned into the *E. coli* vector pGEX3X. Expression of the construct in *E. coli* yielded a GST-$VP16_C$ fusion protein. The fusion protein was purified on a glutathione-Sepharose affinity column and cleaved with factor Xa. The cleavage mixture was purified by glutathione-Sepharose affinity chromatography. This procedure resulted in a protein with three NH_2-terminal residues (Gly-Ile-Pro) derived from the construct, followed by residues 452 to 490 of VP16. Uniformly (>95%) labeled proteins with ^{15}N or with ^{15}N and ^{13}C were obtained by growing the bacteria in minimal medium supplemented with either $^{15}NH_4Cl$ or both $^{15}NH_4Cl$ and [^{13}C]glucose as the sole nitrogen and carbon sources. The labeled proteins were dissolved to 0.5 to 0.9 mM in either 95% H_2O plus 5% ^2H_2O or 99.96% ^2H_2O containing 150 mM KCl, 5 mM perdeuterated DTT, 20 mM perdeuterated tris-AcOH (pH 6.2), and 10 μM EDTA. NMR titrations were carried out by adding unlabeled TAF_{1-140} dissolved in the same buffer. All NMR experiments were carried out at 300 K on a Bruker DMX500 spectrometer equipped with a *z*-shielded gradient triple resonance probe. Quadrature detection in the indirectly detected dimensions was achieved with the time-proportional phase incrementation (TPPI) method. The data were processed with the FELIX software (Biosym Technologies) with appropriate apodization, baseline correction, and zero-filling to yield real 2D 2K × 2K or 3D 512 × 256 × 128 matrices after reduction.
11. The coupling constants were obtained from the ^1H-^{15}N heteronuclear multiple-quantum coherence J-resolved (HMQC-J) spectrum [L. E. Kay and A. Bax, *J. Magn. Reson.* **86**, 110 (1990)].
12. The circular dichroism spectrum of $VP16_C$ alone at 6°C in buffer containing 50 mM phosphate buffer (pH 7.0) and 50 mM NaCl was characteristic for a random-coil structure.
13. The dissociation constant (K_D) of the $VP16_C$-TAF_{1-140} interaction was estimated to be $>10^{-4}$ M in NMR buffer containing 150 mM KCl. The limited solubility of TAF_{1-140} near the actual K_D range precluded accurate determination of K_D.
14. The sequential assignment of the HSQC cross-peaks was achieved by means of the following three-dimensional experiments: ^{15}N-edited nuclear Overhauser effect spectroscopy (NOESY)–HSQC; ^{15}N-edited total correlation spectroscopy (TOCSY)–HSQC; and HN(CO)CA, HNCA, and HCCH-TOCSY [M. Ikura, L. E. Kay, A. Bax, *Biochemistry* **29**, 4659 (1990); L. E. Kay, M. Ikura, R. Tschudin, A. Bax, *J. Magn. Reson.* **89**, 496 (1990); S. Grzesiek and A. Bax, *ibid.* **96**, 432 (1992); A. Bax, G. M. Clore, A. M. Gronenborn, *ibid.* **88**, 425 (1990); L. E. Kay, G. Xu, A. U. Singer, R. Muhandiram, J. D. Forman-Kay, *ibid.* **B101**, 333 (1993)].
15. Chemical shifts of the β protons were determined by NOESY-HSQC and TOCSY-HSQC experiments.
16. Protein-protein interaction assays were performed as in (*9*).
17. GAL4(1–147) and GAL4-VP16 fusions were expressed and purified essentially as described [D. I. Chasman, J. Leatherwood, M. Carey, M. Ptashne, R. Kornberg, *Mol. Cell. Biol.* **9**, 4746 (1989)]. All of the GAL4 fusion proteins had the expected mass, as determined by electrospray ionization mass spectroscopy. Activators (2 pmol) were preincubated with 100 ng of reporter construct pG_5BCAT and HeLa nuclear extract (50 μg) for 20 min at 20°C in a final volume of 30 μl in buffer containing 10 mM Hepes (pH 7.9), 7.5% glycerol, 1 mM DTT, 4 mM $MgCl_2$, 50 mM KCl, 10 mM ammonium sulfate, 1% polyethylene glycol, 0.2 mM PMSF, and bovine serum albumin (100 μg/ml). Transcription was initiated by adding 0.5 mM ribonucleotides and was then allowed to proceed for 30 min at 30°C. After primer extension [B. D. Dynlacht, T. Holey, R. Tjian, *Cell* **55**, 563 (1991)], the products were resolved on a 10% denaturing gel. The DNA binding activities of the GAL4 derivatives were verified by gel electrophoretic mobility shift assays.
18. A. P. Campbell and B. D. Sykes, *Annu. Rev. Biophys. Biomol. Struct.* **22**, 99 (1993).
19. $VP16_{469-485}$ was synthesized on an automated synthesizer and purified by high-performance liquid chromatography. The peptide was determined by electrospray ionization mass spectroscopy to have the expected molecular weight. The peptide was dissolved in 95% H_2O plus 5% ^2H_2O containing 150 mM KCl, 5 mM perdeuterated DTT, 20 mM perdeuterated tris-AcOH (pH 6.2), and 10 μM EDTA, and then the pH of the solution was adjusted to 6.2 by adding dilute KOH. The required amount of concentrated TAF_{1-140} was mixed with the peptide solution. The final concentrations of $VP16_{469-485}$ and TAF_{1-140} were 3 mM and 0.3 mM, respectively. The sequential assignment was obtained by TOCSY, double-quantum filtered correlation spectroscopy (DQFCOSY), and NOESY. In the NOESY spectra, 512 free induction decays were collected with a 5000-Hz sweep width and 2048 points in the F2 dimension, and the spectra were recorded at 300 K with mixing times of 100, 200, and 350 ms.
20. These observations lend credence to an early suggestion that acidic activation domains are α-helical when bound to their targets [E. Giniger and M. Ptashne, *Nature* **330**, 670 (1987)].
21. This perturbation is unlikely to result from indirect effects on the secondary structure of $VP16_C$, because Ala has a higher helical propensity than either Phe or Leu [P. Y. Chou and G. D. Fasman, *Adv. Enzymol. Relat. Areas Mol. Biol.* **47**, 45 (1978)].
22. S. K. Burley and R. G. Roeder, *Annu. Rev. Biochem.* **65**, 769 (1996).
23. M. L. Schmitz *et al.*, *J. Biol. Chem.* **269**, 25613 (1994).
24. P. H. Kussie *et al.*, *Science* **274**, 948 (1996).
25. Y. Lin, M. F. Carey, M. Ptashne, M. R. Green, *Cell* **54**, 659 (1988).
26. M. Zhang and H. J. Vogel, *Biochemistry* **33**, 1163 (1994).
27. We thank B. Dynlacht and J. Ross for helpful advice on transcription assays and S. Wolfe and P. Zhou for discussion about the NMR results. Supported in part by a grant from the Hoffman-La Roche Institute of Chemistry and Medicine and an NSF Presidential Young Investigator Award (G.L.V.); the Leukemia Society of America and the Naito Foundation (M.U.); and the Swiss National Foundation of Scientific Research (O.N.). The NMR spectrometer used in this work was purchased with funding from NSF (CHE93-12233).

18 March 1997; accepted 15 July 1997

Accelerated Aging and Nucleolar Fragmentation in Yeast *sgs1* Mutants

David A. Sinclair, Kevin Mills, Leonard Guarente

The *SGS1* gene of yeast encodes a DNA helicase with homology to the human *WRN* gene. Mutations in *WRN* result in Werner's syndrome, a disease with symptoms resembling premature aging. Mutation of *SGS1* is shown to cause premature aging in yeast mother cells on the basis of a shortened life-span and the aging-induced phenotypes of sterility and redistribution of the Sir3 silencing protein from telomeres to the nucleolus. Further, in old *sgs1* cells the nucleolus is enlarged and fragmented—changes that also occur in old wild-type cells. These findings suggest a conserved mechanism of cellular aging that may be related to nucleolar structure.

The *SGS1* gene of *Saccharomyces cerevisiae* is a member of the RecQ helicase family that includes human *BLM* (mutations in which cause Bloom's syndrome) (*1*), human *RECQL* (*2*), and *WRN* (*3*). Patients with Werner's syndrome contain two mutant alleles of *WRN* and display many symptoms of old age including graying and loss of hair, osteoporosis, cataracts, atherosclerosis, loss of skin elasticity, and a propensity for certain cancers (*4*). Cells isolated from patients with Werner's syndrome divide approximately half as many times in culture as those from normal individuals (*4*).

Department of Biology, Massachusetts Institute of Technology, Cambridge, MA 02139, USA.

Yeast cells lacking topoisomerase III activity (*top3*) are unable to unwind negatively supercoiled DNA efficiently and thus grow extremely slowly. Mutations in *SGS1* were first identified by their ability to suppress the slow-growth phenotype of *top3* strains (*5*); the Sgs1 protein was subsequently shown to interact physically with both topoisomerases II and III (*5–7*). *SGS1* is required for the fidelity of chromosome segregation and the suppression of recombination at the ribosomal DNA (rDNA) array and other loci (*5–7*).

Cell division in *S. cerevisiae* is asymmetric, giving rise to a large mother and a small daughter cell. Mother cells undergo, on average, a fixed number of cell divisions and